SOOT MODELING OF ETHYLENE COUNTERFLOW DIFFUSION FLAMES

W. Pejpichestakul[1,2], A. Frassoldati[1], A. Parente[2], T. Faravelli[1*]
tiziano.faravelli@polimi.it
[1]Politecnico di Milano – Dip. CMIC – p.zza L. Da Vinci, 32 – 20133 Milano – Italy
[2]Université Libre de Bruxelles, Ecole Polytechnique de Bruxelles, Aero-Thermo-Mechanical Laboratory, Avenue F.D Roosevelt, 50 - CP 165/41, 1050 Brussels, Belgium

Abstract
Combustion-generated nanoparticles cause detrimental effects to not only health and environment but also combustion efficiency. A detailed kinetic mechanism employing a discrete sectional model is validated using experimental data obtained in laminar counterflow diffusion flames of ethylene/oxygen/nitrogen (Hwang and Chung, 2001). Two configurations, named Soot formation (SF) and soot formation/oxidation (SFO) flames, are modeled using one-dimensional simulation. Radiative heat losses reduce the maximum flame temperature in the range of 20-60 K and therefore reduce soot volume fraction by ~10%. The model predictions accounting for the radiation effects are quite satisfactory. In SFO flames, the difference of maximum soot volume fraction between the experiment and model is less than 30%. In SF flames, the most considerable discrepancy is observed at the most sooting flame ($x_{O,o}$ = 0.28) in which the model underpredicts the soot volume fraction by a factor of two. In these conditions, the soot particles are not able to reach the stagnation plane as observed in the experiments. This suggests that transport properties of soot particles may require further attention. The effect of soot oxidation shows that the model neglecting oxidation of soot significantly increases soot volume fraction in SFO flames by two folds while SF flames are only marginally affected. Also, the absence of soot oxidation leads to the presence of soot particles in the oxidizer zone where they are not observed experimentally. The successful predictions using the soot model including soot oxidation in SFO flames demonstrate that the reaction rates of the processes involved in soot growth and oxidation are appropriate.

Introduction
Combustion-generated nanoparticles are well-known for their adverse effects on health and environment. In practical applications, the presence of soot particles leads the radiative heat losses and consequently lowers the combustion efficiency [1]. Polycyclic aromatic hydrocarbons (PAHs) are widely accepted as soot precursors, and acetylene plays an essential role in the soot growth processes through the sequential HACA (hydrogen abstraction and acetylene addition) mechanism [2]. In addition, condensation of PAHs and gaseous species on soot particle contributes the soot growth. On the contrary, the oxidations of particles

compete with the soot growth. The oxidation processes include the burnout at the surface of particles mainly by OH radical, and the oxidation-induced fragmentation which is the internal burning induced by the penetration of oxygen molecules into particles [3].

Particulate formation and oxidation have been extensively studied in the past two decades particularly in premixed planar laminar flames. In practical combustors, however, the soot evolution becomes extremely complex due to the interactions between chemistry and turbulence flow environment. To achieve a better understanding of soot formation in turbulent flames, laminar counterflow diffusion flame configuration is a good candidate because of its well-defined boundary conditions that can simplify as one-dimensional simulations and its relevance to flamelet model which is often adopted to model practical industrial scale applications [4].

In this work, detailed kinetic modeling of soot formation in atmospheric laminar counterflow diffusion ethylene/oxygen/nitrogen flames has been performed and compared with the experimental studies by Hwang and Chung (2001) [5]. The validation includes soot formation (SF) and soot formation/oxidation (SFO) flames. The inlet velocities are 19.5 cm/s. For SF flames, the fuel inlet was pure ethylene while oxygen mole fraction of the oxidizer inlet ($x_{O,o}$) was varied from 0.2 to 0.28. For SFO flames, the oxidizer inlet is 90% oxygen in nitrogen while the mole fraction of oxygen in the fuel inlet ($x_{F,o}$) was varied from 0.23 to 0.28.

Model Description and Numerical Simulations

The high temperature gas-phase mechanism consists of 300 species and over 8000 reactions. It implements a C_0-C_3 core mechanism obtained from the H_2/O_2 and C_1/C_2 subsets from Metcalfe et al. [6], C_3 from Burke et al. [7], and heavier fuels from Ranzi et al. [8]. The model describes the pyrolysis and oxidation of wide range hydrocarbon fuels and includes the formation of PAHs up to pyrene. The thermochemical properties were obtained from the ATcT database of Rusic [9] or Burcat's database [10]. For some species that were not available in the aforementioned databases, the thermochemical properties were adopted from group additivity method [11].

A soot model based on a discrete sectional approach is coupled to the gas-phase mechanism to model the evolution from gas-phase to solid particles. The model includes the discretization large PAH and soot particles into 20 sections, considered as lumped-pseudo species called "BINs", with a constant discretization spacing factor of two in terms of carbon atoms. Three hydrogenation levels are considered for each BIN as sub-sections, labeled "A", "B" and "C", which varies from 0.8 for BIN1A to 0.05 for BIN25C. The complete soot mechanism used in this work (POLIMI1800s) has been extensively validated against laminar premixed flames of different fuels in wide range operating conditions which is discussed elsewhere [12]. The successive kinetic mechanism consists of approximately 400

species and 25,000 reactions. Further details of the soot kinetics model are available in [13,14].

All numerical simulations were performed using OpenSMOKE++ suite program by Cuoci et al. [15]. Laminar counterflow diffusion flames 1-D simulations were performed using the mixture-average diffusion coefficient and including thermal diffusion (Soret effect) in species transport equations. Radiative heat losses were accounted using optically thin approximation [16,17]. Solution gradient and curvature coefficients of 0.05 and 0.5 were assigned to ensure the smoothness of the calculated profiles.

Results and Discussions

Figure 1 shows the effects of radiative heat losses on the predicted flame temperatures. The yellow shaded areas represent the sooting region of the two flames. As expected, the radiative heat losses reduce the maximum temperature of all flames in the range of 25-60 K.

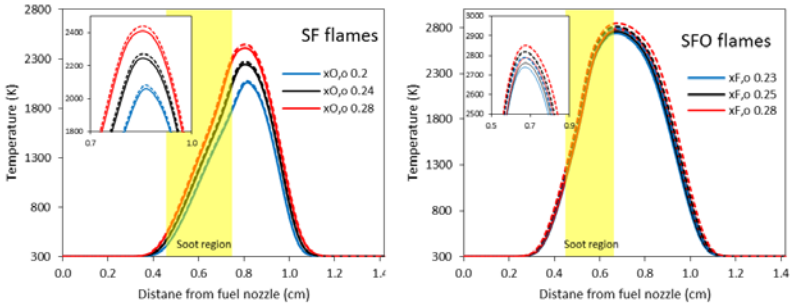

Figure 1. Calculated temperature profiles of SF flames (left panel) and SFO flames (right panel). Dashed lines: model neglecting radiative heat losses. Solid lines: model including radiative heat losses.

Figure 2 shows the comparison of the soot volume fractions profiles between experimental data and model predictions. The model predictions are obtained both including and the neglecting radiative heat losses. The lower temperature reduces soot formation in all flames by approximately 10%. However, the model predictions including radiative heat losses still provide good agreement with the experimental data. It can reproduce the qualitative trends of soot volume fraction peaks that are slightly shifted towards oxidizer zone with the increased oxygen content. Specifically, the model predictions of SFO flames are quite satisfactory, with the discrepancy in maximum soot volume fraction between the model and measurement of less than 30%. The largest differences are observed for SF flames in particular the xO,o = 0.28 flame, the most sooting flame, where the model underpredicts the soot volume fraction by less than a factor of two. In SF flames, the model is not able to capture the particle stagnation plane location well which is resulting from the convection/diffusion of particles towards the stagnation

plane. This suggests the transport properties of soot particles should be investigated further, in particular thermophoresis, which plays a major role in these conditions [18].

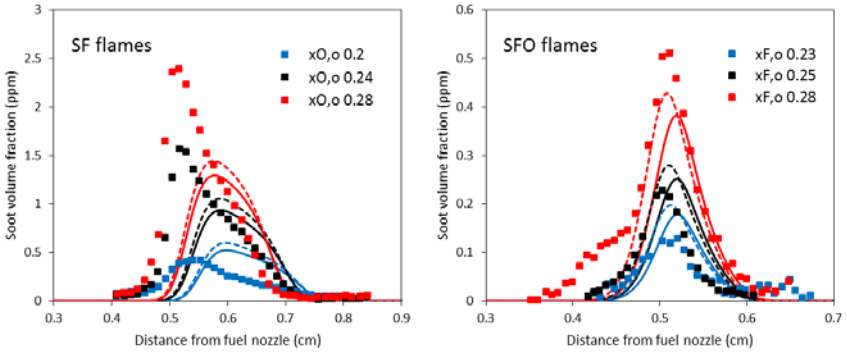

Figure 2. Comparison of soot volume fraction profiles between experimental data (symbol) and model (lines) of SF flames (left panel) and SFO flames (right panel). Dashed lines: model neglecting radiative heat losses. Solid lines: model including radiative heat losses.

To highlight the effect of soot oxidation, Figure 3 shows the effect of soot oxidation on the predicted soot volume fraction in comparison with the measurements. As expected, in SF flames, soot oxidation has marginal effects, since soot particles are pushed away from the sooting region of the flames and are convected towards fuel region. On the contrary, in SFO flames, the removal of particle oxidation increases soot volume fraction drastically by approximately 50%. Additionally, the soot particles are able to form and diffuse towards the oxidizing zone where soot particles are not observed experimentally. The successful predictions using the complete soot model in SFO flames demonstrate that the reaction rates of the processes involved in soot growth and oxidation are appropriate.

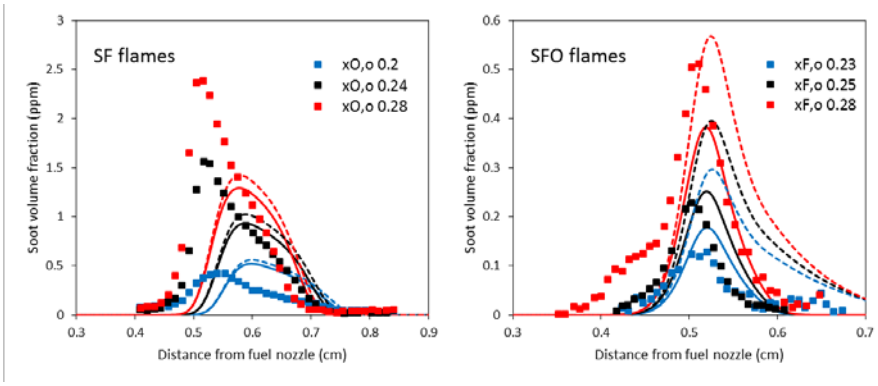

Figure 3. Comparison of soot volume fraction profiles between experimental data

(symbol) and model (lines) of SF flames (left panel) and SFO flames (right panel). Dashed lines: model neglecting soot oxidation. Solid lines: model including soot oxidation.

Conclusions

This work contains the validation of a detailed kinetic mechanism employing a discrete sectional soot model using experimental results from two different laminar counterflow diffusion ethylene flames configurations. Soot formation (SF) and soot formation/oxidation (SFO) flames at different oxygen content have been analyzed. All numerical simulations are performed using one-dimensional simulations considering radiative heat losses.

The inclusion of radiative heat losses lowers the maximum temperature by 25-60 K. The reduction of temperature leads to a lower soot volume fractions in all flames by 10%. Model predictions accounting for radiative heat losses provide good agreement with the experimental data in particular for SFO flames. The difference of maximum soot volume fraction between the experiment and model is less than 30%. In SF flames, the largest discrepancy in soot formation is observed at the most sooting flame conditions ($x_{O,o} = 0.28$) in which the model underpredicts the soot volume fraction by a factor of two. The underprediction of soot volume fraction is evident close to the stagnation plane. These discrepancies show that that the convection and diffusion of particles away from the flame is insufficient. This suggests that transport properties and particularly thermophoresis of soot particles may require further attention.

The effect of soot oxidation is also demonstrated. The model neglecting oxidation of soot significantly increases total soot volume fraction in SFO flames by two folds. On the contrary, SF flames are only slightly affected by soot oxidation. In addition, the absence of soot oxidation leads to the presence of soot particles in the oxidizer zone of SFO flames, where they are not observed experimentally. The successful predictions using the soot model including soot oxidation in SFO flames demonstrate that the reaction rates adopted in this model to describe the processes involved in soot growth and oxidation are appropriate.

Acknowledgement

This project has received funding from the European Union's Horizon 2020 research and innovation programme under the Marie Sklodowska-Curie grant agreement No 643134.

References

[1] Bockhorn, H., D'Anna, A., Sarofim, A.F., Wang, H., "Combustion generated fine carbonaceous particles", 2007

[2] Wang, H., Frenklach, M., "A detailed kinetic modeling study of aromatics formation, growth and oxidation in laminar premixed ethylene and acetylene flames, Combust. Flame". 2180: 173–221 (1997)

[3] Ghiassi, H., Toth, P., Jaramillo, I.C., Lighty, J.S., “Soot oxidation-induced fragmentation: Part 1: The relationship between soot nanostructure and oxidation-induced fragmentation”, Combust. Flame. 163: 179–187 (2016)

[4] Chrigui, M., Gounder, J., Sadiki, A., Masri, A.R., Janicka, J., “Partially premixed reacting acetone spray using LES and FGM tabulated chemistry”, Combust. Flame. 159: 2718–2741 (2012)

[5] Hwang, J.Y., Chung, S.H., “Growth of soot particles in counterflow diffusion flames of ethylene”, Combust. Flame. 125: 752–762 (2001)

[6] Metcalfe, W.K., Burke, S.M., Ahmed, S.S., Curran, H.J., "A hierarchical and comparative kinetic modeling study of C1- C2hydrocarbon and oxygenated fuels”, Int. J. Chem. Kinet. 45: 638–675 (2013)

[7] Burke, S.M., Burke, U., Mc Donagh, R., & Curran, H.J., “An experimental and modeling study of propene oxidation. Part 2: Ignition delay time and flame speed measurements”, Combust. Flame. 162: 296–314 (2015)

[8] Ranzi, E., Frassoldati, A., Grana, R., Cuoci, A., Faravelli, T., Kelley, A.P., Law, C.K., “Hierarchical and comparative kinetic modeling of laminar flame speeds of hydrocarbon and oxygenated fuels”, Prog. Energy Combust. Sci. 38: 468–501 (2012)

[9] Ruscic, B., “Active Thermochemical Tables: Sequential Bond Dissociation Enthalpies of Methane, Ethane, and Methanol and the Related Thermochemistry”, J. Phys. Chem. A. 119: 7810–7837 (2015)

[10] Goos, E., Burcat, A., Ruscic, B., BurcatThermo, (2016). http://garfield.chem.elte.hu/Burcat/burcat.html (accessed May 1, 2017).

[11] Benson, S. W., “Thermochemical Kinetics”, Wiley, New York, 1976.

[12] Pejpichestakul, W., Ranzi, E., Pelucchi, M., Frassoldati, A., Cuoci, A., Parente, A., Faravelli, T., “Soot effect on intermediate pahs concentration in premixed laminar flames”, Proc. Combust. Inst. Submitted (2018)

[13] Saggese, C., Ferrario, S., Camacho, J., Cuoci, A., Frassoldati, A., Ranzi, E., Wang, H., Faravelli, T., “Kinetic modeling of particle size distribution of soot in a premixed burner-stabilized stagnation ethylene flame”, Combust. Flame. 162: 3356–3369 (2015)

[14] Pejpichetsakul, W., Frassoldati, A., Parente, A., Faravelli, T., “Kinetic modeling of soot formation in premixed burner-stabilized stagnation ethylene flames at heavily sooting condition”, Tenth Mediterr. Combust. Symp., Naples, Italy, 2017.

[15] Cuoci, A., Frassoldati, A., Faravelli, T., Ranzi, E., “OpenSMOKE++: An object-oriented framework for the numerical modeling of reactive systems with detailed kinetic mechanisms”, Comput. Phys. Commun. 192: 237–264 (2015)

[16] Grosshandler, W.L., “RADCAL: A Narrow-band Model for Radiation Calculations in a Combustion Environment”, NIST Tech. Note 1402. (1993)

[17] Sazhin, S., “An approximation for the absorption coefficient of soot in a

radiating gas", Fluent Eur. Ltd. (1994)

[18] Stagni, A., Cuoci, A., Frassoldati, A., Ranzi, E., Faravelli, T., "Numerical investigation of soot formation from microgravity droplet combustion using heterogeneous chemistry", Combust. Flame. 189: 393–406 (2018)